



# Analysis of the relationship between urban size and heat island intensity using WRF model

Takebayashi, Hideki  
Senoo, Masashi

---

(Citation)

Urban Climate, 24:287-298

(Issue Date)

2018-06

(Resource Type)

journal article

(Version)

Accepted Manuscript

(Rights)

© 2017 Elsevier B.V.

This manuscript version is made available under the CC-BY-NC-ND 4.0 license  
<http://creativecommons.org/licenses/by-nc-nd/4.0/>

(URL)

<https://hdl.handle.net/20.500.14094/90004948>



Title: Analysis of the relationship between urban size and heat island intensity using WRF model

Authors: Hideki Takebayashi (Kobe University, Japan), Masashi Senoo (The Kansai Electric Power Company, Japan)

Corresponding Author: Hideki Takebayashi, Associate Professor, Dr. Eng., Department of Architecture, Graduate school of Engineering, Kobe University, Rokkodai, Nada, Kobe 657-8501, Japan, Tel. & Fax: +81-78-803-6062, E-mail: thideki@kobe-u.ac.jp

Abstract:

In this study, the relationship between urban size and heat island intensity is analyzed using the meso-scale Weather Research & Forecasting (WRF) model, and is applied to three different sized cities (Tokyo, Osaka, and Nagoya). Given that the urban areas of the study region spread inland, there were a number of high temperature points, with air temperature tending to be relatively higher in Tokyo. The spatial average air temperature in urban areas rise with the expansion of the urban size, since higher air temperature areas increase inland. In the case of calculating the heat island intensity using spatial average temperatures in urban areas, the heat island intensity is related to urban size.

Key Words: Heat island intensity, Urban size, Meso-scale, WRF

The relationship between urban size and heat island intensity is analyzed using WRF model, and is applied to three different sized cities (Tokyo, Osaka, and Nagoya).

The heat island intensities of Osaka and Tokyo were almost the same at the same distance points from the coast regardless of different urban areas.

In the case of calculating the heat island intensity using spatial average temperatures in urban areas, the heat island intensity is related to urban size.

## 1. Introduction

Urban heat island intensity is defined by the air temperature difference between an urban area and its surrounding suburbs. Oke (1973) revealed that urban heat island intensity is proportional to the logarithm of the population, based on observations in a number of cities in North America and Europe. Fukuoka (1983) and Park (1986) both showed the same relationship in Japanese and Korean cities and revealed that the slope of the relationship is steep for cities with more than 300,000 people. Sakakibara and Kitahara (2003) also showed a similar relationship for cities in Nagano Prefecture, Japan; however, the change in slope, such as that found by Fukuoka and Park, was not obtained.

In these studies, population was used to indicate the degree of urbanization. An increase in population, for example, was associated with high-rise buildings and land use change, as well as with an expansion of the urban area. More specific indicators, such as urban area, artificial land coverage, and average building height, should be used to implement more effective heat island countermeasures. The mesoscale Weather Research & Forecasting (WRF) model (Skamarock et al., 2008), which is used generically worldwide, is effective for these studies (Iizuka et al., 2010, Kusaka et al., 2013, Moriyama et al., 2014). Therefore, this study used the WRF model to analyze the relationship between urban size and heat island intensity in three cities representing different sizes (Tokyo, Osaka, and Nagoya). The original definition of urban heat island intensity by Oke (1973) is the annual maximum air temperature difference. However, since the higher air temperature in the summer is noticed socially, which causes the deterioration of the thermal environment in outdoor space and

the increase of energy consumption, the higher air temperature period of summer was selected as the objective period in this study.

Outline of calculations and calculation results are described in chapters 2 and 3. Conclusion is described in chapter 4. The objective of the study is to analyze the relationship between urban size and heat island intensity, by using WRF model. Present land use and potential natural vegetation are set for land use boundary condition.

## 2. Outline of calculations

The objective study areas are shown in Figure 1. The outer square is domain 1 (3 km grid, 360 km square) and the inner filled square is domain 2 (1 km grid, 103 km square). The nesting technique was used in each region. The calculation results of air temperature at 2 m high and wind velocity at 10 m high in domain 2 were used for the analysis. Calculation conditions are shown in Table 1. The period for which calculations were done was from August 1 – 31, 2010. Based on digital national land information (spatial resolution of 100 m) and a normalized vegetation index created from Landsat7 ETM+ data, urban areas were classified into three categories according to the previous study (Kitao et al., 2010): high-rise and high-density, middle-rise and moderate-density, and low-rise and low-density. Present land use and potential natural vegetation in Tokyo, Osaka, and Nagoya are shown in Figure 2. Potential natural vegetation is an ecological concept referring to the vegetation that would be expected given environmental constraints (climate, geomorphology, geology) without human intervention or a hazard event. The concept has been developed in the mid

1950s by phytosociologist Reinhold Tüxen, partly expanding on the concept of climax. Image data was scanned and mapped. Frequency of urban land use at each distance point from the coast is shown in Figure 3. The total number of these land use grids was 3,698 in Tokyo, 1,271 in Osaka, and 1,416 in Nagoya. Frequency of urban land use in the three cities was larger in the coastal area and decreased gradually in the inland area. Urban land use is large in Tokyo as compared to Osaka and Nagoya. In addition, the number of urban land use grids along the coastal area in Nagoya was slightly smaller compared to those for Tokyo and Osaka.

### 3. Calculation results

#### 3.1. Calculation accuracy

“Fine” days and sea breeze conditions were selected according to the conditions listed in Table 2. Only three days, August 25, 26, and 29, contained these weather requirements and were therefore selected. For these days, the calculated values and observed values, which are instantaneous values every hour, are compared using observation station data in domain 2 of Tokyo, Osaka, and Nagoya. The calculation accuracies of air temperature and wind velocity at the Tokyo, Osaka, and Nagoya observatories on August 25, 26, and 29, 2010 are shown in Table 3. **Position of measurement sites is shown in Figure 4.** A comparison of observed and calculated air temperatures at the Tokyo, Osaka, and Nagoya observatories on

August 26, 2010 is shown in Figure 5. For the three cities, calculation accuracy is comparable to previous studies (Kitao et al., 2010 and Moriyama et al., 2014).

### 3.2. Relationship between distance from the coast and air temperature

The relationship between the distance from the coast and air temperature at 15:00 on August 26, 2010 is shown in Figure 6. Many small plots and some large plots indicate calculated values and observed values, respectively. Line is approximated by the quadratic curve for each plot. Air temperature increased as distance from the coast increased, reached its maximum, and then decreased slightly. We analyzed similar relationships from 9:00 to 20:00. Similar trends were confirmed for other times. While air temperature increased as distance from the coast increased in the coastal areas (less than 20 km), air temperature in Tokyo only continued to increase toward its more inland area.

### 3.3. Air temperature distribution under present land use conditions

The calculation results for air temperature at 2m high under present land use conditions in Tokyo, Osaka, and Nagoya at 15:00 on August 26, 2010 are shown in the upper part of Figure 7, and frequency of air temperature for present land use for that time is shown in Figure 8. In the three cities, air temperature was lower in the coastal areas and higher in the inland areas. Number of higher air temperature points in Tokyo was larger than those in the other cities, which are located mainly in the inland areas.

The relationship between wind velocity, altitude and air temperature at 15:00 on August 26, 2010 are shown in Figures 9 and 10. Whereas air temperature was slightly higher when wind speed was slower, it decreased when wind velocity was more than 3.0 m/s, in all three cities. The points where wind velocity is more than 3.0 m/s are located mainly along the coastal areas. Air temperature was slightly lower at higher altitudes in all three cities. Overall, altitude was not a dominant factor for air temperature in these urban areas.

#### 3.4. Air temperature distribution under natural vegetation land use conditions

The calculation results for air temperature at 2m high under natural vegetation land use conditions in Tokyo, Osaka, and Nagoya at 15:00 on August 26, 2010 are shown in the lower part of Figure 7. Frequency of air temperature for present land use and natural vegetation at 15:00 on August 26, 2010 are shown in Figure 11. The air temperature differences between current urban land uses and natural vegetation means urban heat island phenomena are caused by urbanization. Characteristics of air temperature distribution in natural vegetation land use are the same as those in urban land use, and frequency of air temperature for natural vegetation land use is 1 - 2 °C lower than it is in present land use. Characteristics of air temperature distribution are recognized regardless of the presence of an urban area. A number of high temperature points exist because urban areas spread inland where air temperatures tend to be relatively higher in Tokyo.

#### 3.5. Relationship between distance from the coast and heat island intensity

The relationship between distance from the coast and heat island intensity is shown in Figure 12. In Figure 12a, the approximate curve was extracted from Figure 6. Air temperature near the coast, where the distance from the coast is 0 km, was used as a reference ( $T_r$ ). The approximate curve for Tokyo overlaps the curve for Osaka but does not overlap the curve for Nagoya. The reason for this difference is that less urban land use occurs along the coastal area in Nagoya compared to the coastal areas of Tokyo and Osaka. According to the general urban boundary layer theory, heat island intensity is proportional to the square root of the distance from the urban boundary (the coast), as shown in Figure 12 b. The urban boundary layer is not very developed due to less urban land use along the coastal area of Nagoya, in comparison to Tokyo and Osaka. A schematic diagram of Osaka and Tokyo is shown in Figure 12c. The heat island intensities ( $T_u - T_r$ ) of Osaka and Tokyo were almost the same (Osaka: +2.8 degrees and Tokyo: +3.0 degrees at 20 km from the coast) at the same distance points from the coast regardless of different urban areas. Spatial average heat island intensity in the whole city ( $T_{u\_mean} - T_r$ ) and maximum heat island intensity ( $T_{u\_max} - T_r$ ) are larger as the urban area, which is related to urban surface size and population size (number of inhabitants), increases (Osaka: +2.1, +2.8 degrees, Tokyo: +2.8, +3.7 degrees, respectively).

#### 4. Conclusion

In this study, the relationship between urban size and the heat island intensity is analyzed using the meso-scale Weather Research & Forecasting (WRF) model, and is applied to three different sized cities (Tokyo, Osaka, and Nagoya). Air temperature increased as distance from the coast increased, reached its maximum, and then decreased slightly. Number of higher air temperature points in Tokyo was larger than those in Osaka and Nagoya, which are located mainly in the inland areas. Given that the urban areas of the study region spread inland, there were a number of high temperature points, with air temperature tending to be relatively higher in Tokyo. The heat island intensities of Osaka and Tokyo were almost the same at the same distance points from the coast regardless of different urban areas. The spatial average air temperature in urban areas rise with the expansion of the urban size, since higher air temperature areas increase inland. In the case of calculating the heat island intensity using spatial average temperatures in urban areas, the heat island intensity is related to urban size, which is also related to population size (number of inhabitants). This was proven by lower temperatures correlating with less developed urban land and boundary layer in the coastal area of Nagoya, in comparison with Tokyo and Osaka.

Acknowledgment: This work was supported by JSPS KAKENHI Grant Number 16H04464.

## References

Fukuoka, Y., 1983. Physical climatological discussion on causal factors of urban temperature, *Memories of the Faculty of Integrated Arts and Sciences, Hiroshima University*, Ser. IV, 8, 157-178.

Iizuka, S., Kinbara, K., Kusaka, H., Hara, M., Akimoto, Y., 2009. An attempt to project a future thermal environment in the Nagoya metropolitan area combined with pseudo global warming data , *Proc. Seventh International Conference on Urban Climate*.

Kitao, N., Moriyama, M., Nakajima, S., Tanaka, T., Takebayashi, H., 2009. The characteristics of urban heat island based on the comparison of temperature and wind field between present land cover and potential natural land cover, *Proc. Seventh International Conference on Urban Climate*.

Kusaka, H., Hara, M., Takane, Y., 2012. Urban climate projection by the WRF model at 3-km horizontal grid increment: Dynamical downscaling and predicting heat stress in the 2070's August for Tokyo, Osaka, and Nagoya metropolies. *J. Meteor. Soc. Japan.*, 90B, 47-63.

Moriyama, M., Inui, Y., Takebayashi, H., 2014. Study on Thermal Environmental Mitigation Effects Caused by Changes of Urban Form on a Large Scale Area, *Proc. 7th Japanese-German Meeting on Urban Climatology*.

Oke, T. R., 1973. City size and the urban heat island, *Atmospheric Environment*, 7, 769-779.

Park, H.C., 1986. Features of the heat island in Seoul and its surrounding cities, *Atmospheric Environment*, 20, 1859-1866.

Sakakibara, Y., Kitahara, Y., 2003. Relationship between Population and Heat Island Intensity in Japanese Cities, *Tenki*, 50, 625-633.

Skamarock, W. C., Klemp, J. B., Dudhia, J., Gill, D. O., Barker, D. M., Duha, M. G., Huang, X. Y., Wang, W., Powers, J. G., 2008. A description of advanced research WRF version 3, NCAR/TN-475+STR.

#### List of tables

Table 1 Calculation conditions

Table 2 Criteria for “fine” day and sea breeze condition classifications

Table 3 Calculation accuracy of air temperature and wind velocity for the Tokyo (left), Osaka (center), and Nagoya (right) observatories on August 25, 26, and 29, 2010

#### List of figures

Figure 1 Objective study areas

Figure 2 Present land use and potential natural vegetation in Tokyo, Osaka, and Nagoya

Figure 3 Frequency of urban land use at each distance point from the coast (left: number, right: integral number)

**Figure 4 Position of measurement sites**

Figure 5 Comparison of observed and calculated air temperatures at the Tokyo (left), Osaka (center), and Nagoya (right) observatories on August 26, 2010

Figure 6 Relationship between distance from the coast and air temperature at 15:00 on August 26, 2010

Figure 7 Calculation results for air temperature at 2m high in Tokyo, Osaka, and Nagoya at 15:00 on August 26, 2010

Figure 8 Frequency of air temperature in the current land use grids at 15:00 on August 26, 2010

Figure 9 Relationship between wind velocity and air temperature at 15:00 on August 26, 2010

Figure 10 Relationship between wind altitude and air temperature at 15:00 on August 26, 2010

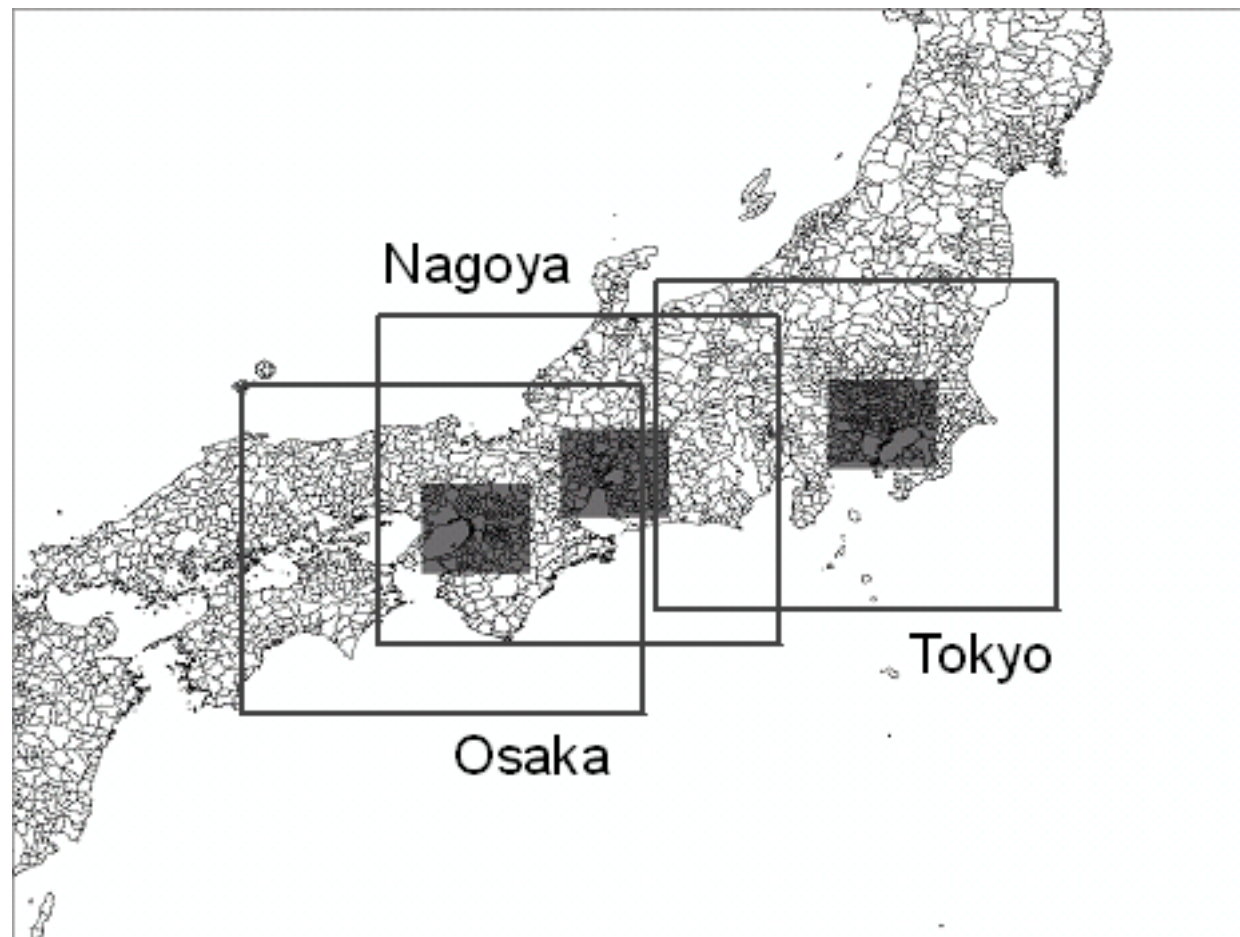
Figure 11 Frequency of air temperature for present land use and natural vegetation at 15:00 on August 26, 2010

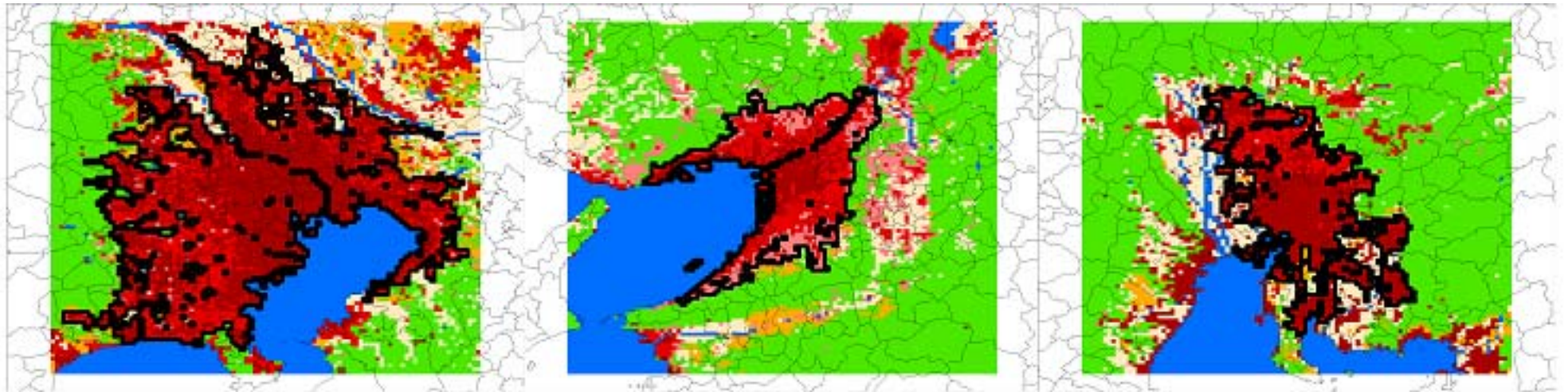
Figure 12 Relationship between distance from the coast and heat island intensity a. approximation by quadratic equation, b. approximation by  $1/2$  power equation, and c. schematic diagram for Osaka and Tokyo

a. Approximation by quadratic equation

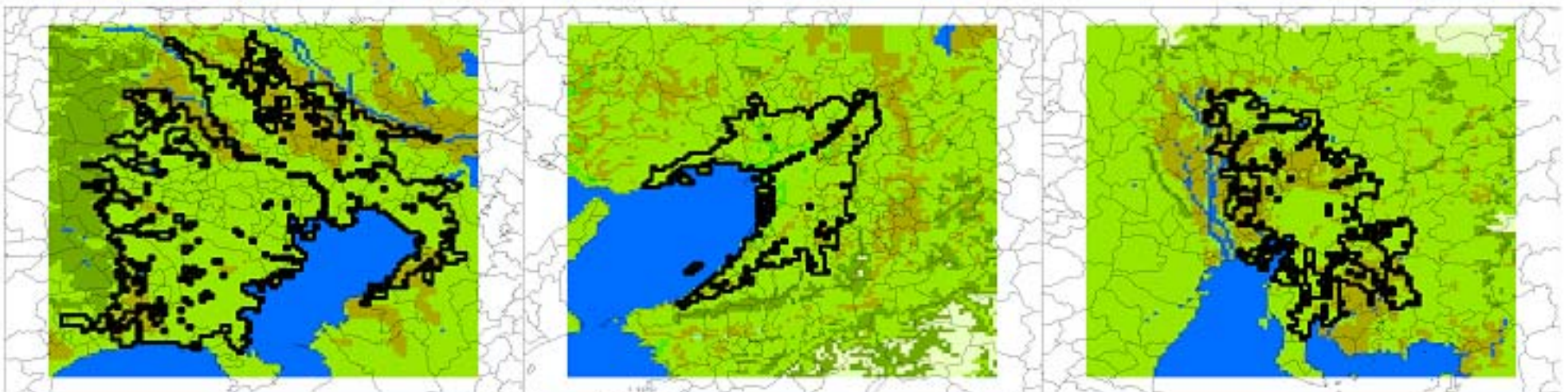
b. Approximation by  $1/2$  power equation

c. Schematic diagram for Osaka and Tokyo





Present land use



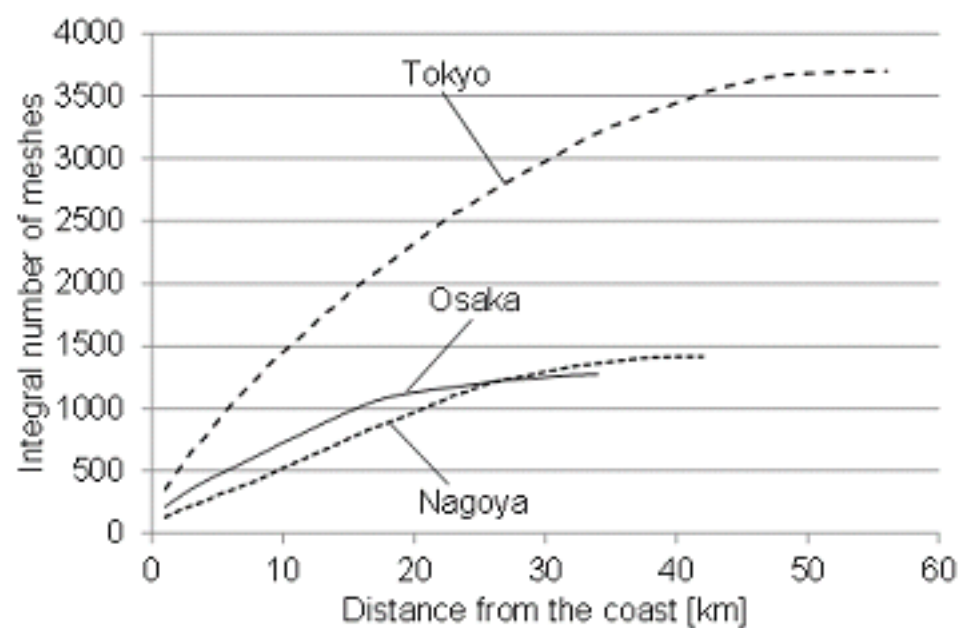
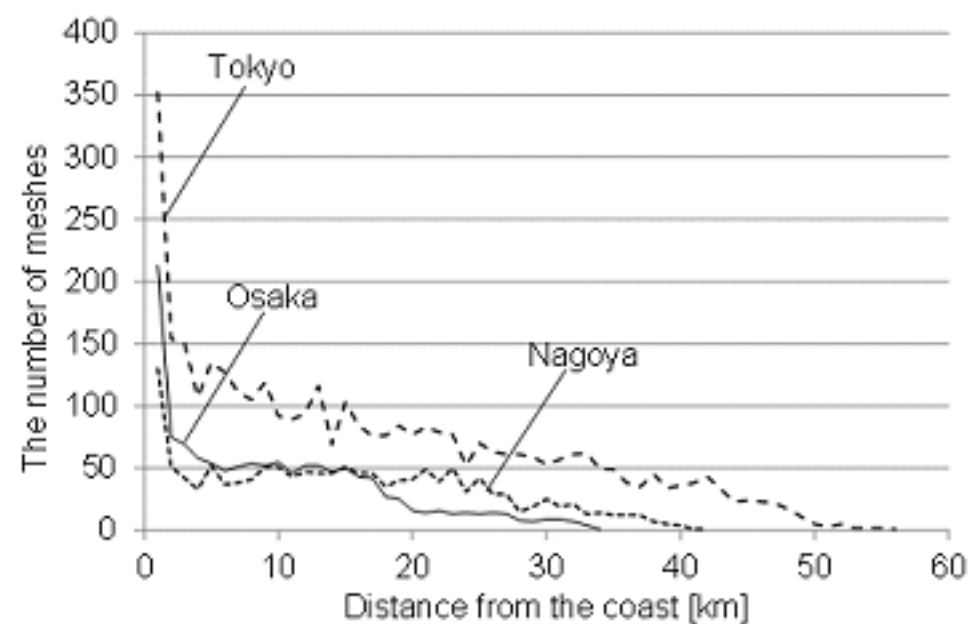
Potential natural vegetation

Tokyo

Osaka

Nagoya

■: urban, ■: drying cropland and pasture, ■: irrigated cropland and pasture, ■: grassland, ■: mixed forest, ■: water bodies, ■: wooden wetland, ■: barren or sparsely vegetated





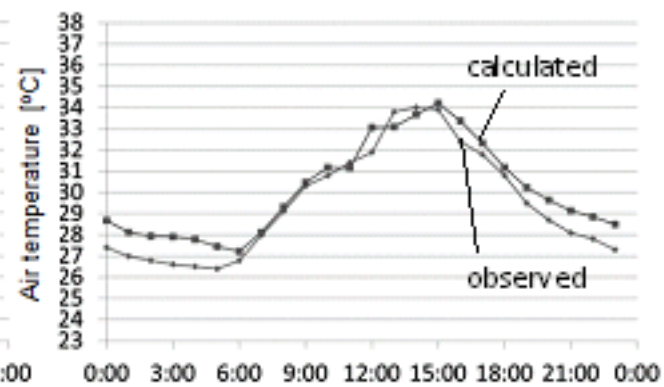
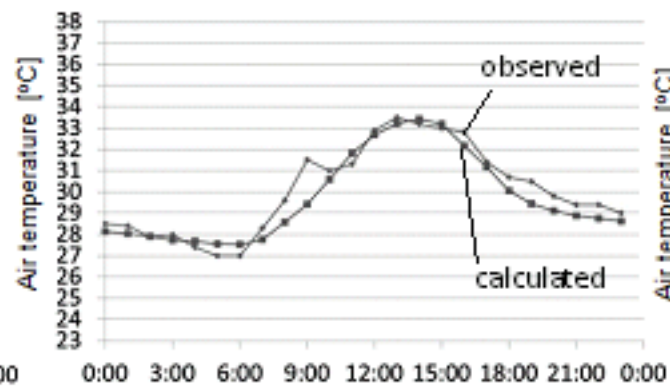
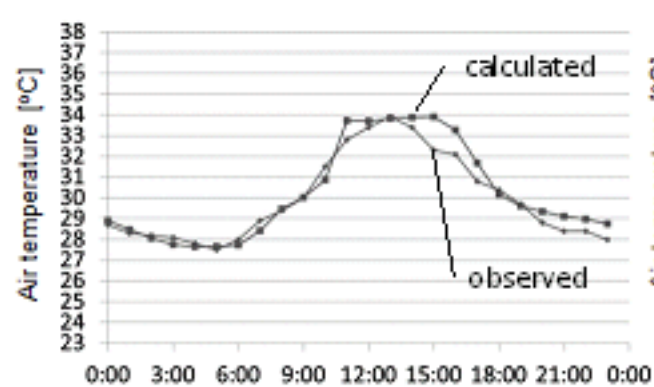
Tokyo

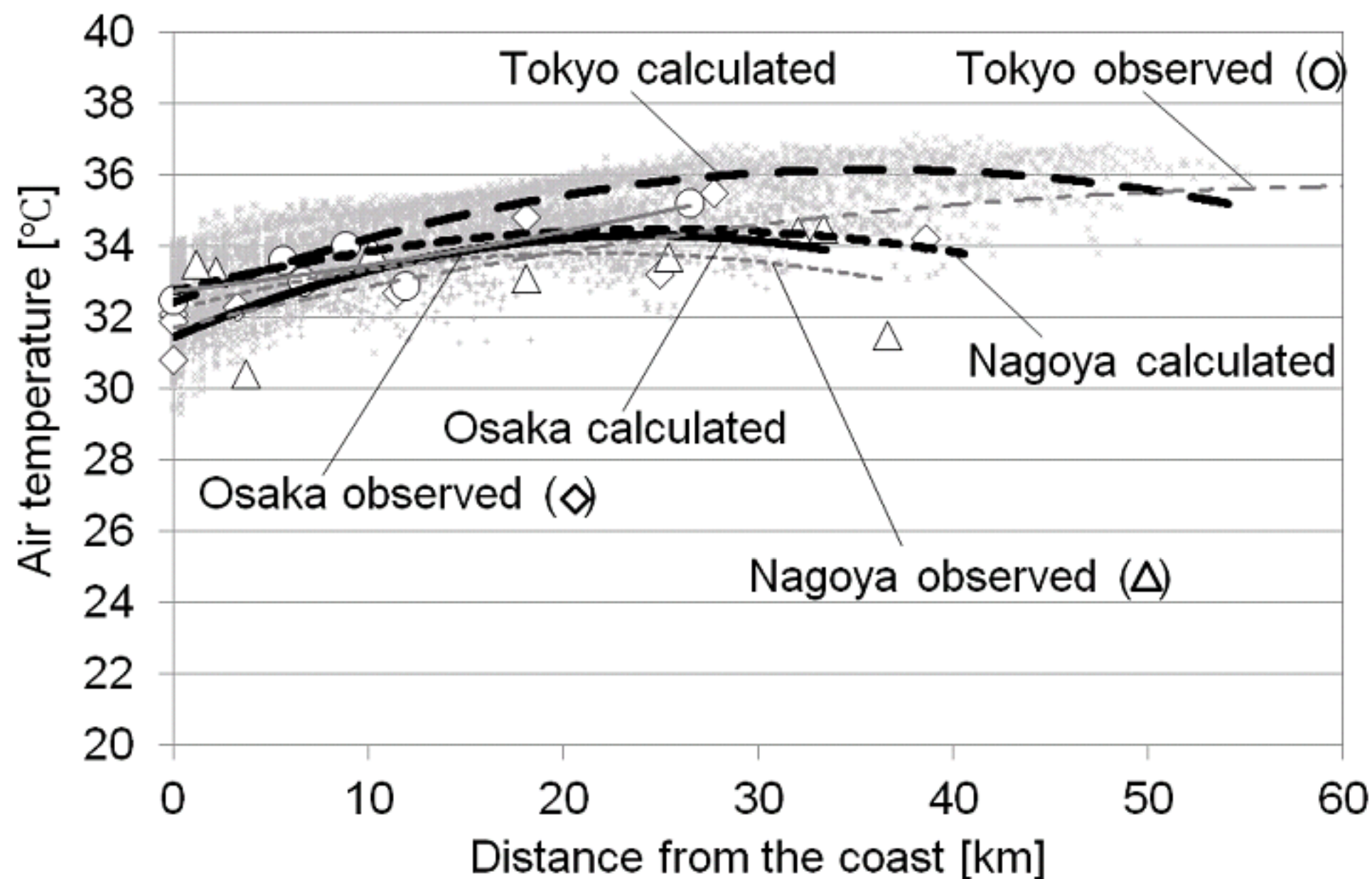


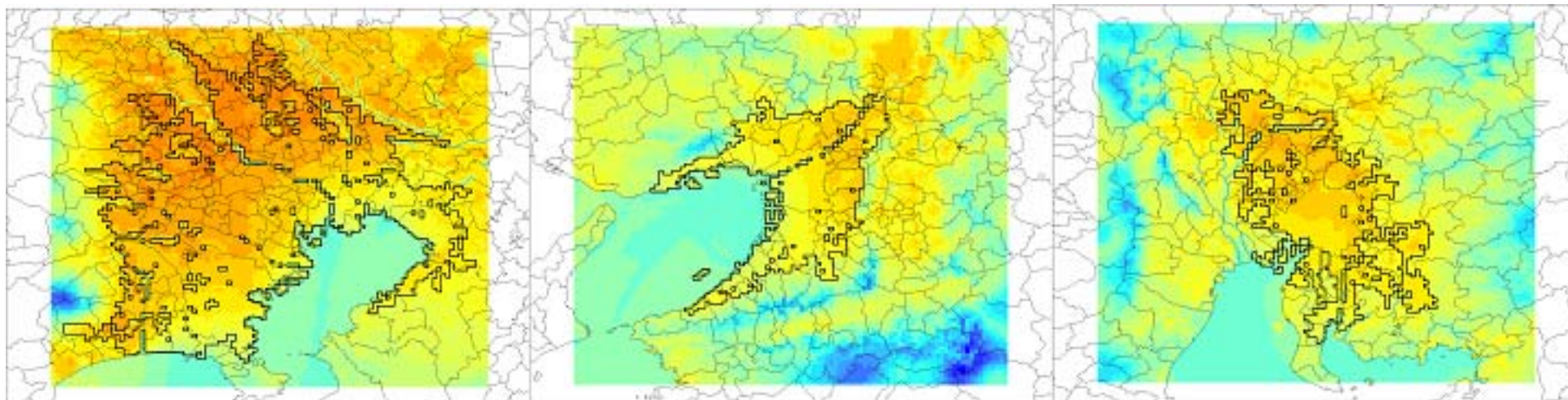
## Osaka



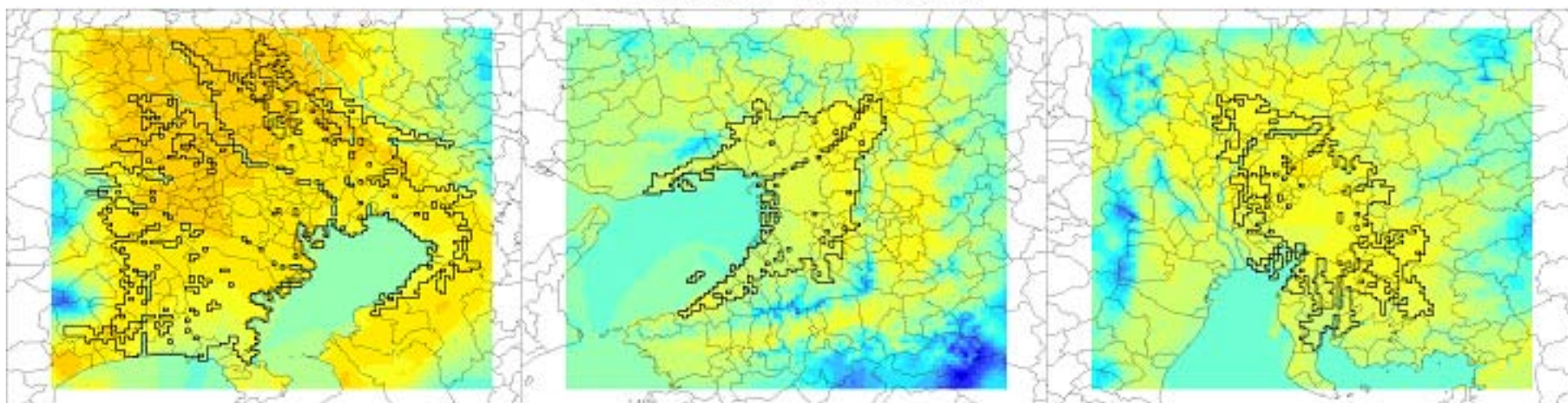
## Nagoya







Present land use

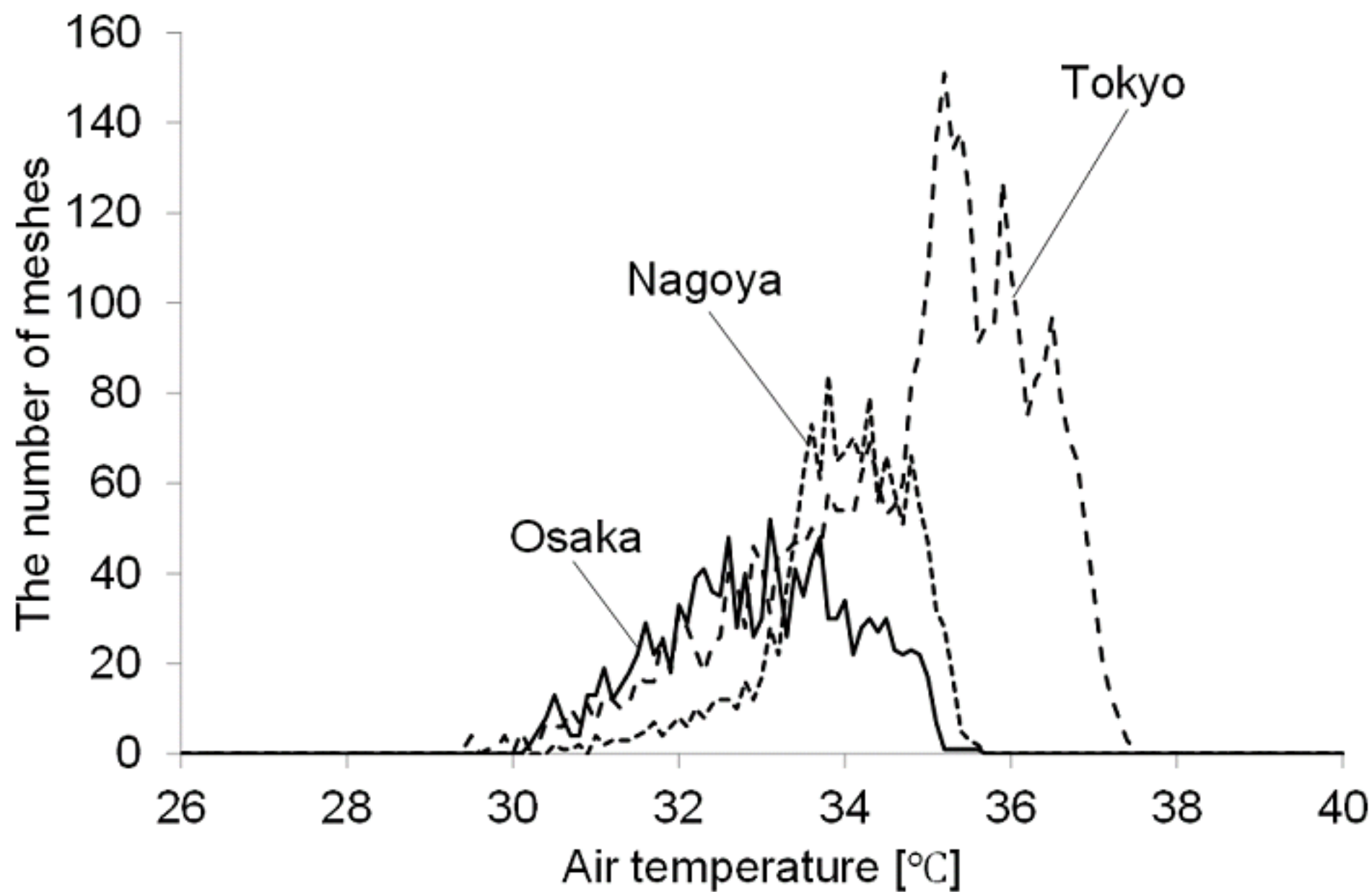


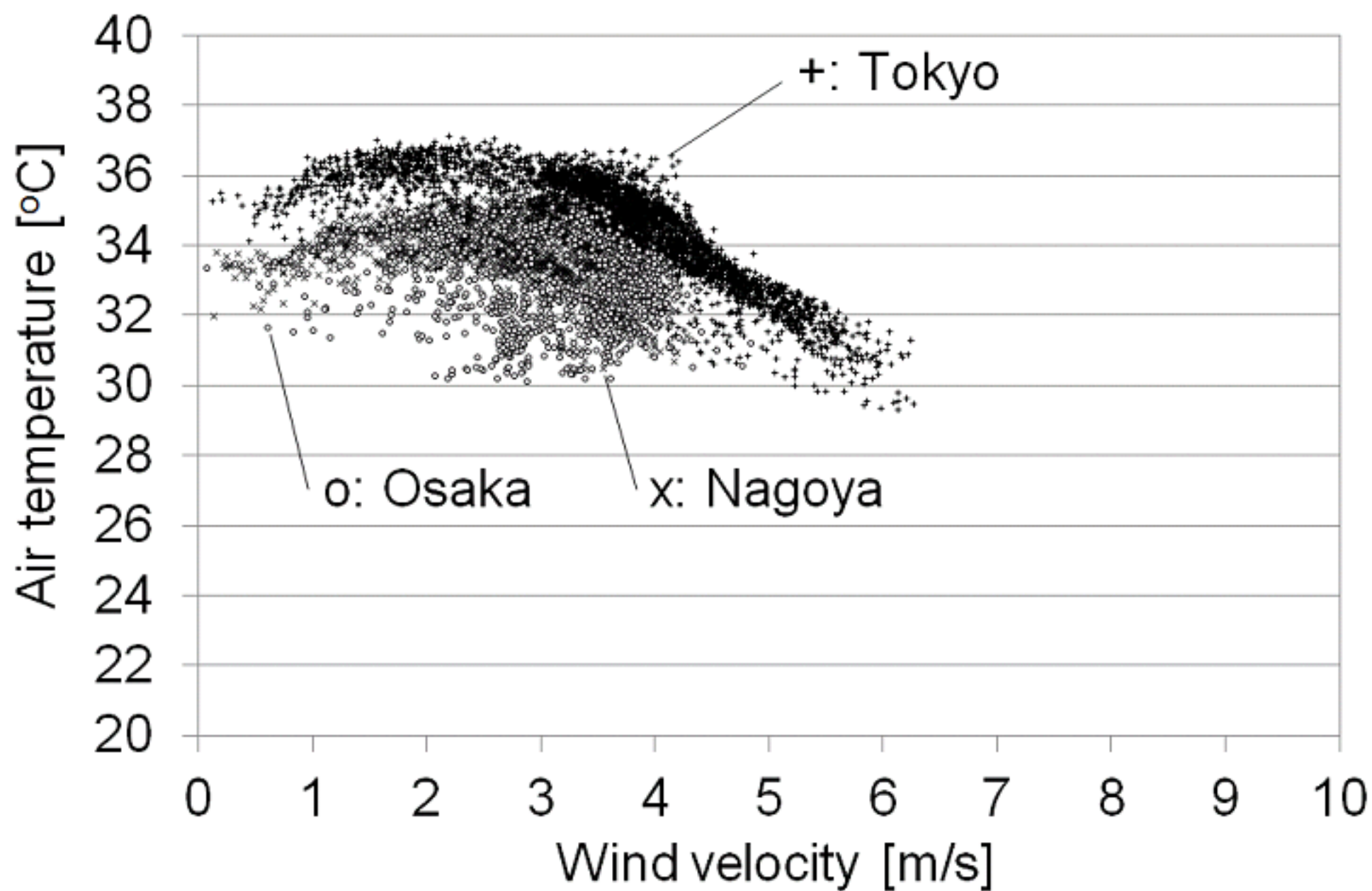
Potential natural vegetation

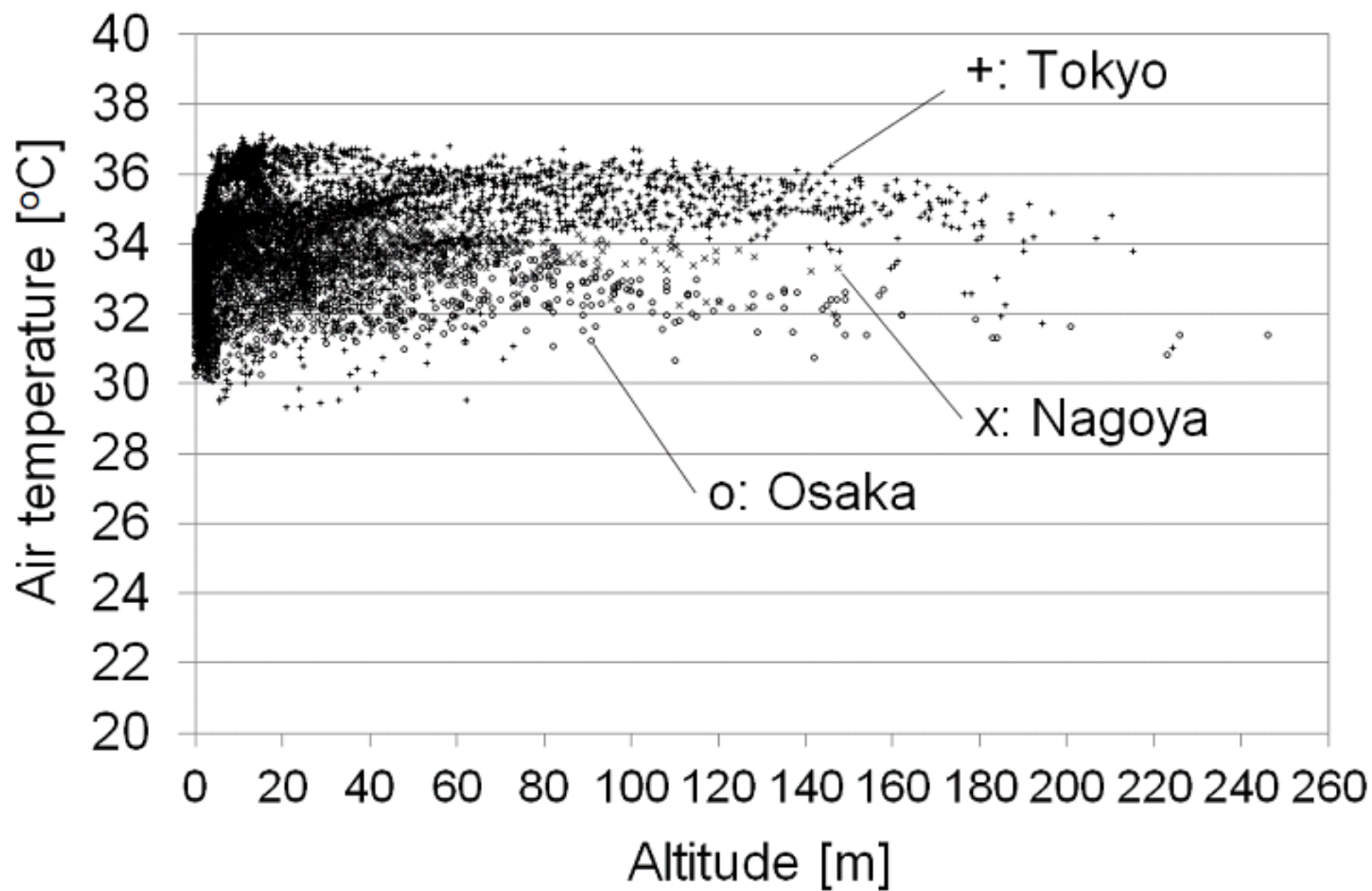
Tokyo

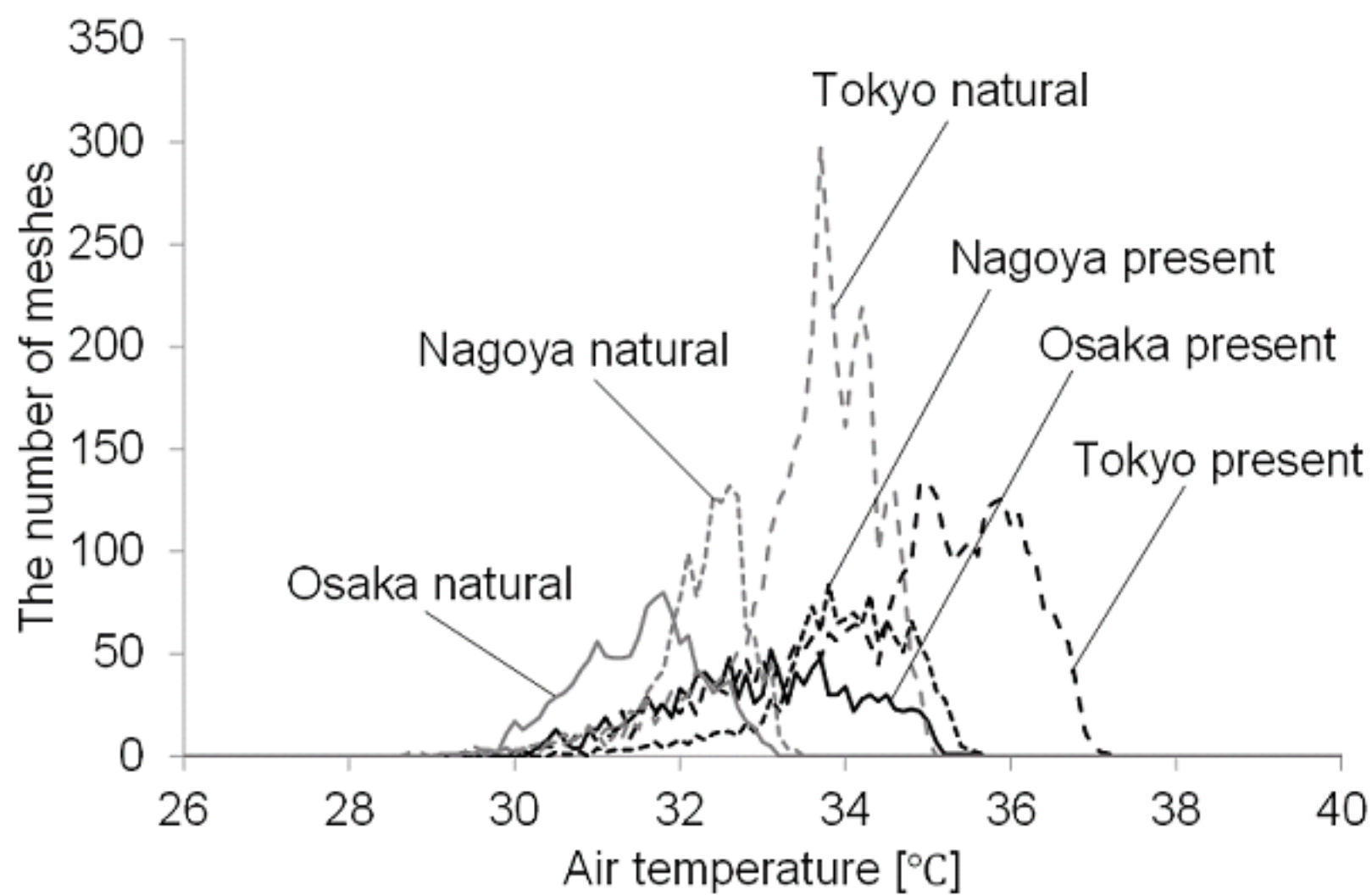
Osaka

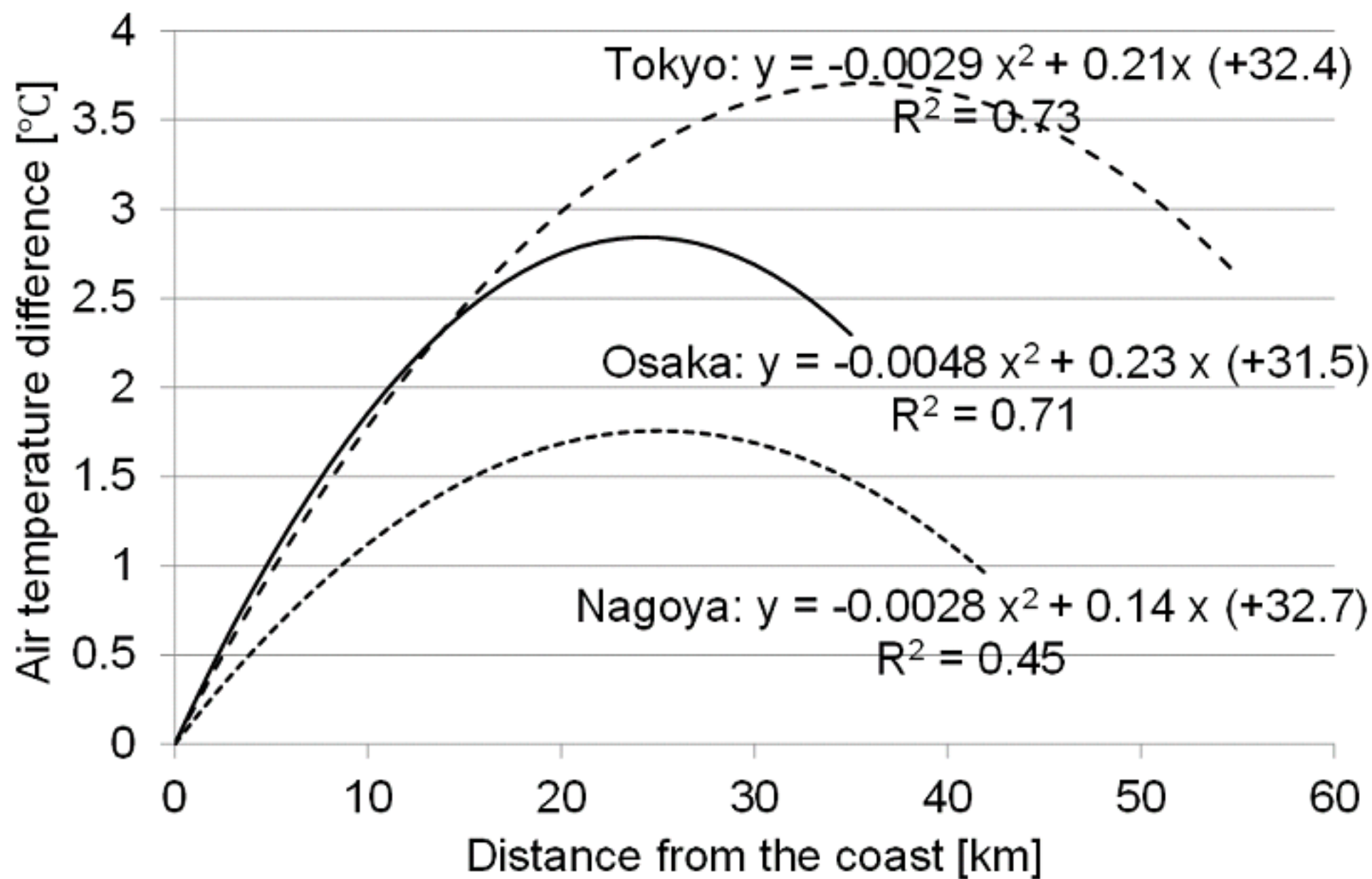
Nagoya

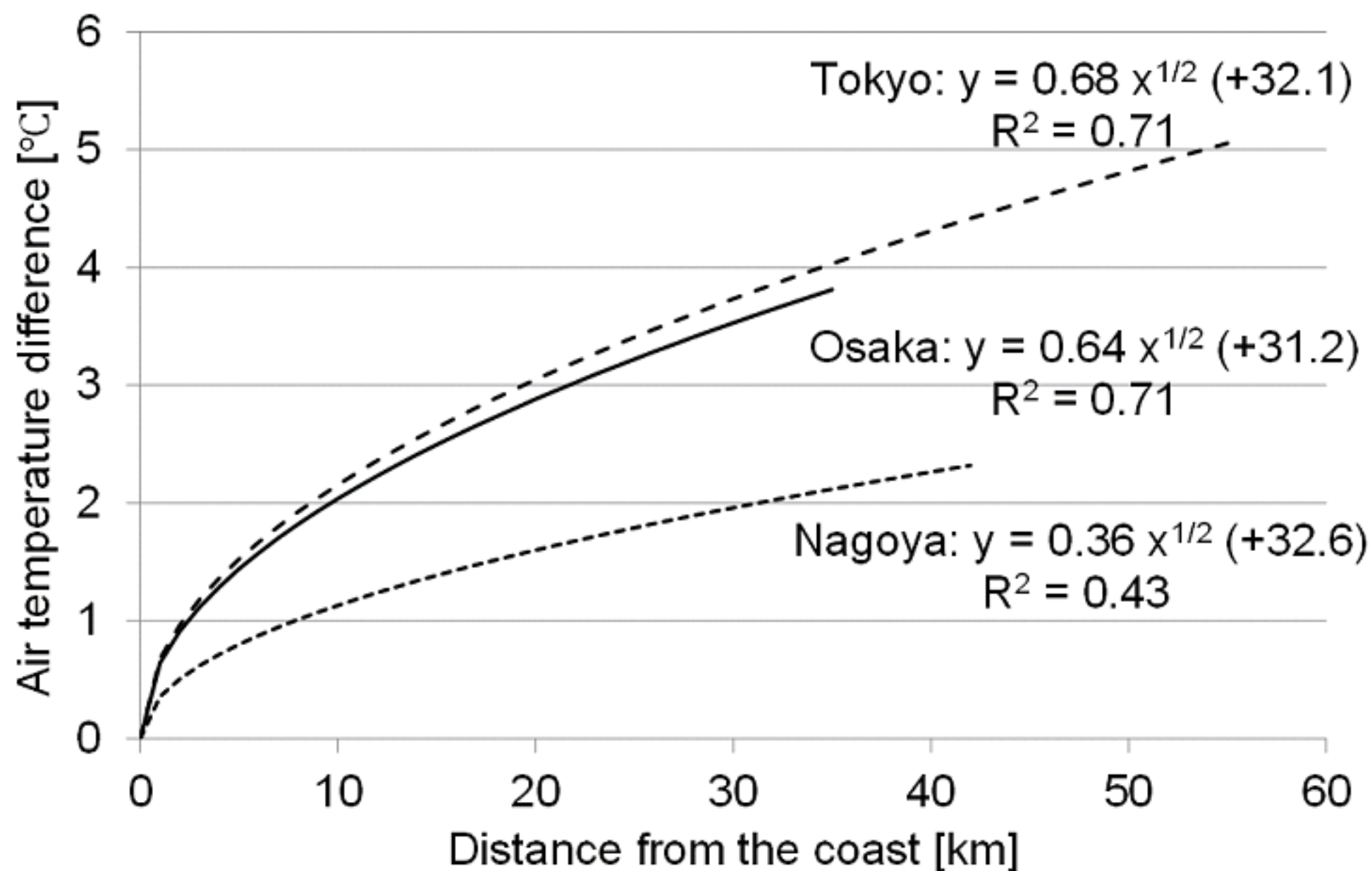




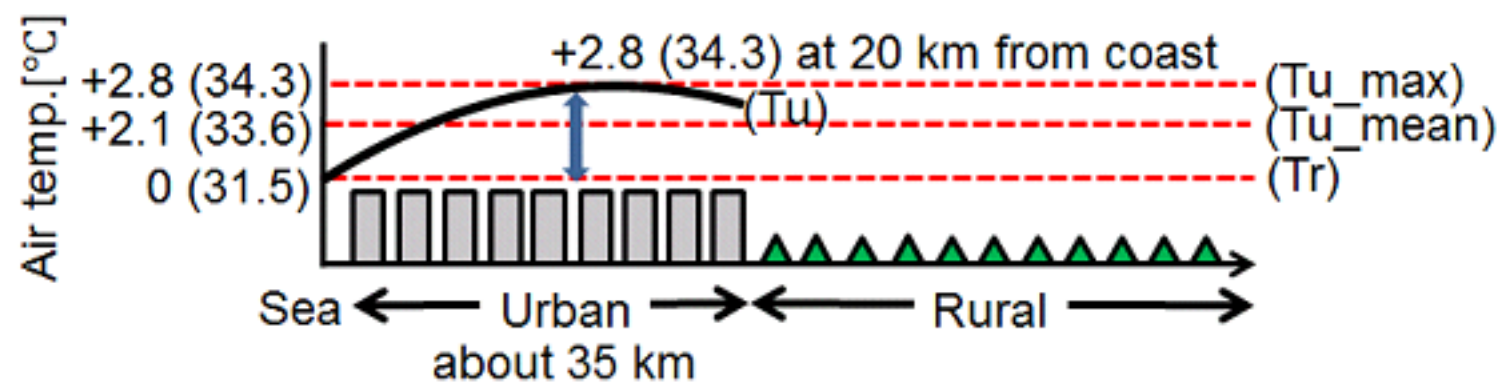




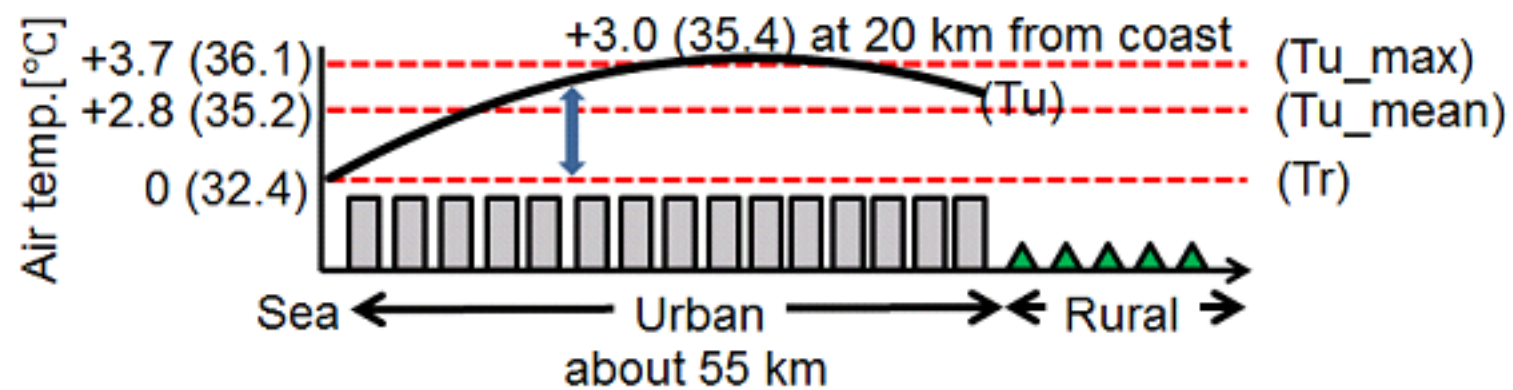




Osaka



Tokyo



Period	August 1 - 31, 2010
Vertical grid	28 layers (ground surface to 100 hPa)
Horizontal grid	Domain 1: 3 km (120 x 120 grid) Domain 2: 1 km (103 x 103 grid)
Objective analysis data	JMA - MANAL, NECP - FNL
Elevation	Digital map (50m x 50m grid)
Land use	Digital national land information (100m x 100m grid), Landsat7 ETM+ data
Microphysics	Purdue Lin et al.
Radiation scheme	RRTM (long wave), Dudhia (short wave)
PBL scheme	Mellor-Yamada-Janjic
Surface scheme	Urban: UCM (Urban Canopy Model) Non Urban: Noah LSM
Cumulus parameterization	None
FDDA	None

Fine day	Criteria	Sea breeze condition	Criteria
Weather	Mostly Sunny and Sunny	Wind velocity	More than 2.0 m/s at Observatory
Sunlight hours	More than 7.0 hours	Wind direction	Tokyo: S, SSW Osaka: W, WSW Nagoya: SSE, SE
Solar radiation	More than 19 MJ/m <sup>2</sup>	Duration time	More than 6 hours under the above conditions
Precipitation	Less than 0.5 mm		

Air temperature at 2m high in Tokyo

Observation station	Bias [ $^{\circ}\text{C}$ ]	RMSE [ $^{\circ}\text{C}$ ]	Correlation [-]
Tokyo	0.27	0.50	0.92
Nerima	0.40	0.96	0.91
Fuoyu	1.91	2.22	0.88
Saitama	0.74	1.02	0.95
Tsukuba	0.62	1.07	0.95
Chiba	-0.47	0.56	0.97

Air temperature at 2m high in Osaka

Observation station	Bias [ $^{\circ}\text{C}$ ]	RMSE [ $^{\circ}\text{C}$ ]	Correlation [-]
Osaka	-0.22	0.45	0.95
Kobe	-0.07	0.47	0.92
Sakai	0.08	0.83	0.93
Toyonaka	-0.12	0.70	0.94
Yao	0.97	1.32	0.92
Hirakata	0.04	0.87	0.93

Air temperature at 2m high in Nagoya

Observation station	Bias [ $^{\circ}\text{C}$ ]	RMSE [ $^{\circ}\text{C}$ ]	Correlation [-]
Nagoya	0.52	0.85	0.93
Tokai	0.13	1.02	0.93
Aisai	-0.31	0.75	0.94
Toyota	0.52	1.14	0.96
Gifu	0.49	0.95	0.93
Tajimi	0.26	1.70	0.94

Wind velocity at 10m high in Tokyo

Observation station	Bias [m/s]	RMSE [m/s]	Correlation [-]
Tokyo	-0.73	0.96	0.77
Nerima	1.07	1.28	0.28
Fuoyu	-0.27	0.93	0.50
Saitama	0.34	0.68	0.53
Tsukuba	-0.07	0.67	0.54
Chiba	-1.28	1.46	0.51

Wind velocity at 10m high in Osaka

Observation station	Bias [m/s]	RMSE [m/s]	Correlation [-]
Osaka	-0.19	0.69	0.80
Kobe	-1.22	1.42	0.78
Sakai	-0.12	0.74	0.64
Toyonaka	-0.21	0.78	0.72
Yao	-1.15	1.45	0.59
Hirakata	0.64	1.01	0.14

Wind velocity at 10m high in Nagoya

Observation station	Bias [m/s]	RMSE [m/s]	Correlation [-]
Nagoya	-0.60	1.01	0.65
Tokai	0.44	0.68	0.54
Aisai	1.22	1.60	0.52
Toyota	0.06	0.57	0.18
Gifu	-0.68	0.83	0.72
Tajimi	0.18	0.74	0.23